

Article

Coordinate Optimization of the Distribution Network Electricity Price, Energy Storage Operation Strategy, and Capacity under a Shared Mechanism

Wenxia Liu ¹, Shu Wang ^{1,*}, Ye Chen ¹, Xingliang Chen ², Shuya Niu ¹ and Zongqi Liu ¹

¹ State Key Laboratory of Alternate Electrical Power System with Renewable Energy Sources, North China Electric Power University, No. 2 Beinong Road, Changping District, Beijing 102206, China; lwxia@ncepu.edu.cn (W.L.); 18811558093@163.com (Y.C.); 18701676036@163.com (S.N.); lzq@ncepu.edu.cn (Z.L.)

² State Grid Jilin Electric Power Company, Changchun 130000, China; jlecxl@163.com

* Correspondence: wangshufire@163.com

Received: 26 April 2017; Accepted: 19 June 2017; Published: 21 June 2017

Abstract: The large scale deployment of renewable generation is generally seen as the most promising option for displacing fossil fuel generators. A challenge in integrating renewable energy resources (RERs) for distribution networks is to find approaches that ensure the long term sustainability and economic profit of the Distribution Company (DisCo). In this paper, considering the air condition load demand side response, a coordinate optimization of the energy storage capacity and operation strategy is presented to maximize the economic profit of the DisCo. The operation strategy in the optimization is divided into two parts. Under the normal state, a price-based air condition quick response strategy is proposed, with both the comfort and economic efficiency of the users taken into account. Under the fault state, a sharing strategy of Generalized Demand Side Resources (GDSRs) is proposed to improve the utilization level of equipment based on the reliability insurance. Finally, the optimization is carried out on an improved IEEE-33 bus test system. The simulation results verify the effectiveness of the proposed method and discuss the effect of the load demand response participation rate on energy storage configuration. At the same time, the effect of GDSRs on the safe load rate of the line is also presented. The research provides a reference for the optimization and utilization of GDSRs.

Keywords: sharing strategy; generalized demand side resources; aircondition response; energy storage optimization

1. Introduction

The usage of sustainable energy is increasing by a large margin because of fossil fuel exhaustion problems [1]. For example, there are a large number of distributed wind generation (DWG) and solar photovoltaic (PV) components integrated into distribution networks [2]. However, the output of distributed generation (DG) is usually influenced by the climate environment, which is intermittent, uncertain, and fluctuant. Therefore, the operation of distribution networks and the economic profit of the DisCo has been badly affected [3,4]. As important resources available for distribution networks, GDSRs contain energy storage and a demand side response. It can make the interaction between the grid side and the demand side become more flexible [5]. In view of this, learning how to make full use of GDSRs in the planning stage is beneficial to the promotion of both the application of sustainable energy in distribution networks and the DisCo operation efficiency.

Currently, energy storage is expected to become a fundamental element of electricity infrastructure, thanks to its ability to decouple generation and demand over time [6]. For the dispatch strategy of

energy storage, Reference [7] proposed an original scheduling approach for the optimal dispatch of energy storage in modern distribution networks based on fuzzy rules. For the configuration of energy storage, scholars have pursued a lot of research on the optimization of the energy storage configuration, especially during the situation in which the DisCo configures energy storage. In Reference [8], aimed at a single feed, researchers analyzed the positive effects of an energy storage operation strategy on distribution networks when the grid is under the normal state, including the peak shaving capacity, voltage quality, and active power adjustment capacity, and studied the multi-objective optimization of the energy storage capacity. In Reference [9], based on Reference [8], researchers transferred the positive effects into the economic benefit of the DisCo. According to the method of economic characteristics optimization, researchers put forward an energy storage capacity optimization method to maximize the DisCo comprehensive benefits. On the basis of the research above, in Reference [10], researchers analyzed the contribution of energy storage to the reliability of distribution networks under the fault state. Considering the energy storage operation strategy, researchers proposed a joint optimization method of the energy storage operation parameters and the configuration capacity.

As the interaction between supply and demand, the demand side response can change users' inherent mode of power consumption effectively, alleviate the imbalance between supply and demand, and improve the economic efficiency of distribution networks operation [11]. So, it is an important resource to improve the economic benefit of the DisCo. The demand side response can be treated as a power source (i.e., the effect of load reduction) that actively participates in the planning and operation of distribution networks. It is pointed out in Reference [12] that the rational consideration of the impact of the demand side response in planning would help to improve the overall effectiveness of the planning result. In Reference [13], researchers pointed out that the air condition is an important resource of the load demand side response, especially for commercial users. In Reference [14], considering the coordinated operation of PV and energy storage, researchers put forward the configuration model of the energy storage capacity. Additionally, it is shown that the DisCo can improve the economic benefits by considering the demand response in the planning stage. However, in distribution networks energy storage configuration, the demand response for the air condition load is mostly based on an incentive-based response. However, the potential of the price-based response, which does not need the DisCo to pay economic compensation, has not yet been excavated.

In summary, as GDSRs, the energy storage and load demand side response support new ideas for the development of distribution networks planning and operation with the configuring of intermittent energy. Based on interconnected feeders, this paper proposes a coordinate optimization of the energy storage capacity and operation strategy considering the air condition load demand side response. The operation strategy in the optimization is divided into two parts. Under the normal state, a price-based air condition quick response strategy is proposed, with both the comfort and economic efficiency of users taken into account. Under the fault state, a sharing strategy of Generalized Demand Side Resources (GDSRs) is proposed to improve the utilization level of equipment based on the reliability insurance. Finally, aimed at maximizing the economic benefits of the DisCo, this paper carries out the joint optimization of the demand-side electricity price, energy storage operation strategy, and capacity.

The rest of this paper is organized as follows. Section 2 gives the output model of GDSRs under the normal and fault state of distribution networks. The optimization of the electricity price, energy storage operation strategy, and energy storage capacity is introduced in Section 3. The solution of the planning model based on an operation simulation is shown in Section 4. The simulation of the proposed model for testing and the suggestions for the DisCo are provided in Section 5. Finally, Section 6 is devoted to the conclusions.

2. GDSRs Output Model in the Normal and Fault State of Distribution Networks

In this paper, some users in the interconnected feeders are equipped with a decentralized, small-capacity PV. Additionally, they participate in the load demand side response to improve the economic efficiency by using the split-type inverter air condition. Meanwhile, the DisCo constructs

the energy storage and carries out an active operation to enhance the distribution networks economic efficiency and equipment utilization with the friendly load in distribution networks. Based on the above scene, the GDSRs in this paper include energy storage and the friendly load in distribution networks [15].

In order to improve the utilization rate of the equipment and eliminate the redundant equipment configuration in distribution networks, this paper fully explores the value of GDSRs under the fault state. Thus, the classification of the GDSRs model is shown in Figure 1.

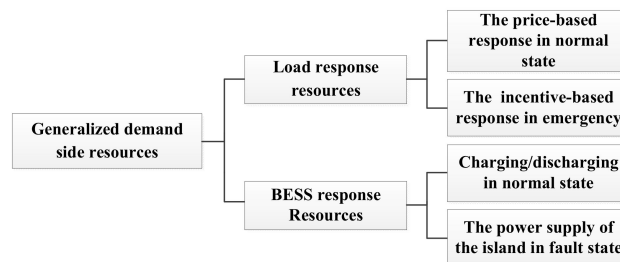


Figure 1. The classification of the GDSRs model.

2.1. Air Condition Load Demand Side Response Model Based on Auto—DR

2.1.1. Air Condition Load Demand Side Response Realization Mode

In order to fully tap the potential and responsiveness of users' side load response and to overcome the "response fatigue" problem caused by a frequent response, the Auto-DR concept [16] was proposed internationally. Based on Auto-DR, this paper presents a functional model of the Users Side Response Terminal (USRT). The function of USRT includes receiving the real-time demand-side electricity price, users' comfortable needs, and the temperature information, regulating the air condition in real-time through the normal and fault state of decision-making modes. The specifics of the workflow are shown in Figure 2:

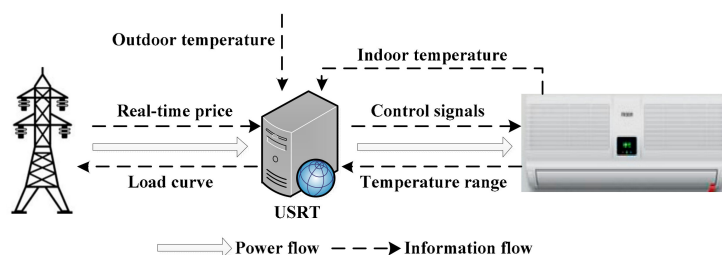


Figure 2. The workflow of USRT.

2.1.2. Price-Based Air Condition Response Model under the Normal State

Under the normal state of distribution networks, USRT adjusts the air condition output according to the demand-side electricity price and temperature fluctuations. The adjustment is aimed at improving the economic efficiency of users on the basis of the protection of users' comfort. Based on the heuristic sliding time window algorithm [17], this paper puts forward a price-based air condition response model considering the limitation of USRT computing resources. The main idea is as follows.

The data window in this paper is composed of multiple response periods. First, determine the candidate air condition output of the first response period in the data window, and the standard is whether it can meet all of the temperature requirements in the data window. Then, choose the best economic efficiency in the candidate output as the output of the response results in the first period. Next, slide the data window in turn to complete the response of all periods.

The authors assume 0.5 h as a response period. Since the indoor temperature has heat storage characteristics, the current period of the air condition output has an impact on the indoor temperature of the current period and next period. Thus, two adjacent response periods in this paper form a data window. Next is the specific response process.

- (1) **Data initialization:** Load the data of array L , demand-side electricity price array C , the PV power output P_v , the users' comfortable demand for indoor temperature $[T_{in}^{\min}, T_{in}^{\max}]$, and outdoor temperature array T_{out} in the data window.
- (2) **Determine the air condition candidate stalls meeting the temperature requirements:** Assuming that the current response time is the k -th time period, calculate the air condition power stalls for the k -th period which meets the users' temperature requirements in the k -th period, according to Equivalent Thermal Parameters model (ETP model) of the air condition heat exchanging process [18], and then form array Q_k . Pointing at each element $Q_k(m)$ in Q_k , calculate the optional power stalls for the $k + 1$ period to meet the users' temperature requirement in the $(k + 1)$ -th period when the k -th air condition power stalls are set to $Q_k(m)$, and then form the array $Q_{m,k+1}$. If there are no stalls meeting the users' temperature requirement in the $(k + 1)$ -th period when the k -th air condition power stalls are set to $Q_k(m)$, delete $Q_k(m)$ from array Q_k . The calculation formula of the ETP model is shown in (1).

$$T_{in}^{k+1} = (T_{out}^{k+1} \pm qPR\eta)(1 - e^{-\frac{\Delta k}{RC}}) + T_{in}^k e^{-\frac{\Delta k}{RC}} \quad (1)$$

In the formula, T_{in} represents the indoor temperature, °C. T_{out} represents the outdoor temperature, °C. Δk represents the time interval in the simulation. R represents the thermal resistance parameter, °C/W. C represents the equivalent heat capacity parameters, J/°C. P represents the rated cooling/heating power of air condition, kW. η represents the performance parameters of the air condition. q represents the five power stalls of the air condition, which includes stop, 25% activate, 50% activate, 75% activate, and fully activate, and in these five states, q means 0, 0.25, 0.5, 0.75, 1, respectively.

- (3) **Calculate the average electricity price of the data window when the air condition power stalls are $Q_k(m)$ in the k -th period:** According to the price of the k -th period and $(k + 1)$ -th period, the output of the users' PV and the optional power stalls array $Q_{m,k+1}$ for the $(k + 1)$ -th period, the average electricity price of the data window when the air condition power stalls are $Q_k(m)$ in the k -th period is marked as $C_a^k(m)$ in (2).

$$C_a^k(m) = \frac{[Q_k P - P_v(k)]C(k) + [\frac{1}{n} \sum_{i=1}^n Q_{m,k+1}(i)P - P_v(k+1)]C(k+1)}{[Q_k(j)P - P_v(k)] + [\frac{1}{n} \sum_{i=1}^n Q_{m,k+1}(i)P - P_v(k+1)]} \quad (2)$$

In the formula, $C(k)$, $C(k + 1)$ represent the price of the k -th and $(k + 1)$ -th periods, respectively. $P_v(k)$, $P_v(k + 1)$ represent the users' PV output of the k -th and $(k + 1)$ -th periods, respectively. n represents the number of elements of $Q_{m,k+1}$.

- (4) **Select the best stall in the best position:** Select the stall with the lowest average price of the data window as the k -th period optimal stalls.

The decision-making process ensures that the result of the response meets the temperature requirement of the users' comfortable needs, and maximizes the economic benefits of the users' participation in the load demand side response, so that it is in line with USRT design positioning.

2.1.3. Incentive-Based Air Condition Response Model in the Fault State

In order to fully exploit the contribution of the load demand side resource under the fault state, the incentive-based air condition response strategy in this paper is: when there is load transfer in the feeders group, the air condition of users who participate in the response project in advance is interrupted. Under this strategy, the DisCo is responsible for interrupting the air condition, so the DisCo needs to provide economic compensation to the users according to the time of the air condition disconnection [19]. The specific calculation method of economic compensation is shown in (3).

$$C_{i.comp} = \sum_{j=1}^{N_{transfer}} P_i r_j R_a \frac{\lambda_j}{\lambda_j + \mu_j} \quad (3)$$

In the formula, $C_{i.comp}$ represents the amount of financial compensation received by the i -th user. $N_{transfer}$ represents the amount of elements when they are in fault, where the i -th user needing to be transferred or belonging to the feeder needs to accept the transfer load. P_i represents the rated power of the i -th user's air condition. r_j represents the average duration of the j -th element failure. R_a represents the lack of a power supply evaluation rate. λ_j, μ_j represent the failure rate and repair rate of the j -th element, respectively.

2.2. Energy Storage Operation Strategies in the Normal and Fault State

When one feeder of the interconnected feeders fails, the dispatch of energy storage and demand side resources of the feeders can reduce the standby for each feeder and effectively improve the utilization rate of the distribution network equipment. Accordingly, this paper presents the strategies of energy storage under the normal and fault state as follows.

Under the fault state of distribution networks, when the faulty element is located within the planned island, the energy storage can supply power to the load in the planned island by releasing power to reduce the power failure [20]. When the faulty element is located outside the planned island, the energy storage in the feeders group can take the transfer load by releasing power. It can reduce the load capacity prepared for the transfer load and the redundancy of distribution networks.

Under the normal state of distribution networks, the reasonable energy storage discharging and charging strategy is key to reducing the peak and valley difference of the load curve and improving the economic efficiency of the DisCo [21]. The effect of some strategy is reducing the peak and valley difference of the load curve. The effect of the other strategy is arbitrage through charging when the transmission grid electricity price is low and discharging when the transmission grid electricity price is high. Considering the combined effect, this paper puts forward a new strategy, which is mainly to track the users' load fluctuations and is supplemented with tracking the transmission price fluctuations, to expand the utilization depth of energy storage.

Specifically, when the load fluctuation is detected to be less than the load tracking lower limit $P_{k.min}$, the energy storage stores power. When the load fluctuation is detected to be more than the load tracking upper limit $P_{k.max}$, the energy storage releases power. When the load fluctuation is more than $P_{k.min}$ and less than $P_{k.max}$, the energy storage traces the transmission grid price. It means that when the transmission grid price is lower than the price tracking lower limit C_{min} , the energy storage stores power, and when the grid price is higher than the price tracking upper limit C_{max} , the energy storage releases power, or the energy storage is in the floating state. The specific calculation formula of the load tracking and electricity price tracking limits are shown in (4).

$$\begin{aligned} X_{k.max} &= \frac{\sum_{i=1}^n X_i}{n} + k_{max} \left(Max_x - \frac{\sum_{i=1}^n X_i}{n} \right) \\ X_{k.min} &= \frac{\sum_{i=1}^n X_i}{n} + k_{min} \left(Min_x - \frac{\sum_{i=1}^n X_i}{n} \right) \end{aligned} \quad (4)$$

In the formula, X represents the user load l and the transmission grid price C . $X_{k_{\max}}$ and $X_{k_{\min}}$ indicate $P_{k_{\max}}$ and $P_{k_{\min}}$ when X represents the user load l , respectively. $X_{k_{\max}}$ and $X_{k_{\min}}$ indicate C_{\max} and C_{\min} when X represents the transmission grid price C , respectively. N indicates the total number of selected statistical points. Max_x and Min_x represent the maximum and minimum values of the user load or the transmission grid price, respectively. k_{\max} and k_{\min} represent the proportional parameters set by the upper and lower thresholds, respectively, including the transmission grid price upper limit parameter $k_{c_{\max}}$, transmission grid price lower limit parameter $k_{c_{\min}}$, user load upper limit parameter $k_{l_{\max}}$, and user load lower limit parameter $k_{l_{\min}}$.

It is worth noting that in order to ensure energy storage has enough power for the island load and the transfer load power supply when the distribution networks are in fault, the lower limit of state of charge (SOC) needs to be set as $Soc_{t,\min}$. At the same time, because of the physical characteristics of energy storage, the upper limit of SOC needs to be set as $Soc_{t,\max}$. Energy storage can only charge and discharge when the SOC meets the restrictions above. In summary, the specific process of energy storage charging and discharging strategy under the normal state is shown in Figure 3:

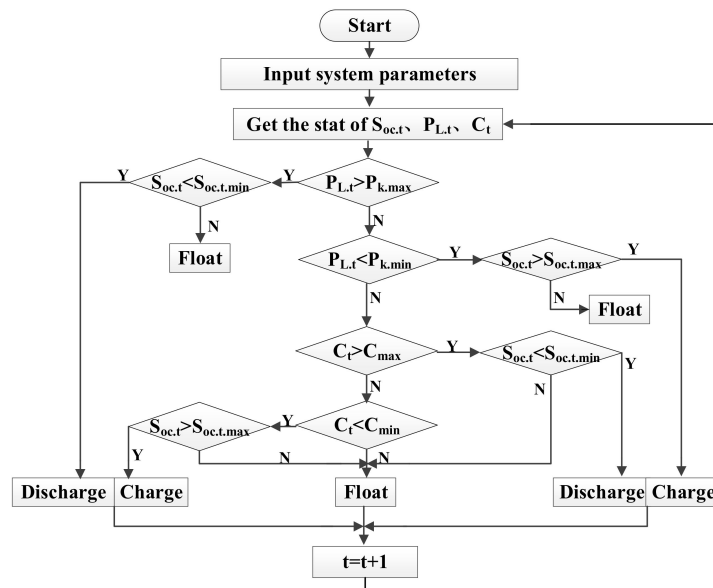


Figure 3. Operation strategy of energy storage.

3. Optimization of Electricity Price, Energy Storage Operation Strategy, and Energy Storage Configuration

In this paper, the contribution to the reliability and safety load rate of the line (the upper limit of the line load rate on the normal state under the influence of accepting the transfer load on the fault state) are converted to economic benefits. Through the optimal configuration of energy storage and the coordinated operation of GDSRs, the economic benefits of distribution networks are maximized. The demand-side electricity price affects the shape of the load curve. The operating strategy of energy storage under the normal state determines the effectiveness of energy storage. The utility of energy storage and the shape of the load curve affect the result of energy storage configuration. Therefore, in this paper, the electricity price, configuration parameters of energy storage, and the operation parameters $k_{c_{\max}}$, $k_{c_{\min}}$, $k_{l_{\max}}$, $k_{l_{\min}}$, and SOC_{\min} of energy storage are set as the optimization variables and optimized jointly.

3.1. Objective Function

The maximization of the DisCo economic benefits can be expressed as maximizing the differences between the incremental income and incremental cost caused by the configuration of GDSRs. The

incremental cost derives from the total life cycle cost of energy storage and the compensatory cost to the users when distribution networks interrupt the power supply of the air condition. Incremental income comes from both the normal and fault state. Their specific categories are shown in Figure 4.

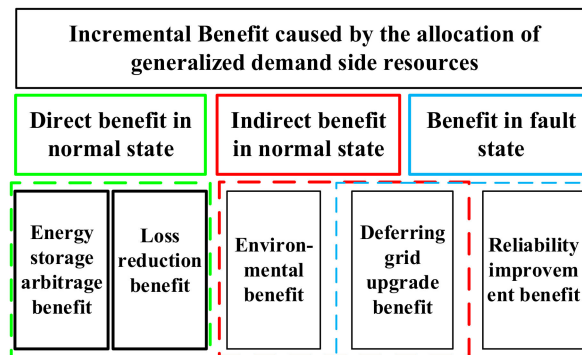


Figure 4. The classification of distribution network company incremental benefit.

Thus, the objective function is shown in (5).

$$\max F(k_{c,\max}, k_{c,\min}, k_{l,\max}, k_{l,\min}, SOC_{\min}, S_{es}, P_{es}) = B_{dir} + B_{del} + B_{env} + B_{rel} - C_{tol} - C_{dsm} \quad (5)$$

In the formula, F represents the net income for the DisCo. B_{dir} represents the direct return of the DisCo. B_{del} represents the profit of delaying the upgrading of distribution networks. B_{env} represents the environmental benefits. B_{rel} represents the profit of reliability improvement. C_{tol} represents the life cycle cost of energy storage. C_{dsm} represents the compensatory cost for the users when distribution networks interrupt the power supply of the air condition, which is shown in Formula (3). $k_{c,\max}$, $k_{c,\min}$, $k_{l,\max}$, and $k_{l,\min}$ are the operation parameters of energy storage. SOC_{\min} is the lower limit of SOC. S_{es} , P_{es} are the rated capacity and power of energy storage, respectively.

In Reference [10], based on a single feeder, the research put forward the calculation method of the revenue model of the DisCo. When the load demand side response, the generalized demand side sharing mechanism in the feeders group, and the connection of lines inside the isolated island are considered, the calculation methods of the direct return, environmental benefits, and energy storage life cycle cost do not change. However, the profits calculation of delaying the upgrading of distribution networks and reliability improvement is no longer applicable. Thus, this paper follows the calculation method of the direct income, environmental benefits, and energy storage equipment life cycle cost in the reference, and then puts forward the profits calculation method of delaying the upgrading of distribution networks and reliability improvement as follows.

3.1.1. The Profits of Delaying the Upgrading of Distribution Networks

Under the normal state, the coordinated dispatching of GDSRs in the feeders group reduces the peak and valley difference of the load curve. Under the fault state, the coordinated dispatching of GDSRs in the feeders group increases the safety load rate of the line. Take the feeders group shown in Figure 5 as an example. To ensure that the networks meet the 'N-1' safety guidelines, which means that the line load of both sides can be fully transferred on the fault state, the safety load rate of the line should be set to 50% before GDSRs allocation. As shown in Figure 5, after the feeders group configured with GDSRs, energy storage can afford the transfer load by releasing power when A1 is in fault. At the same time, the load demand side response can also reduce the transfer load by the incentive-based air condition response. Therefore, the amount of transfer load that A2 accepting reduces, which makes the line load rate of A2 under the normal state, can be more than 50%. In other words, the safety load rate of the line increases.

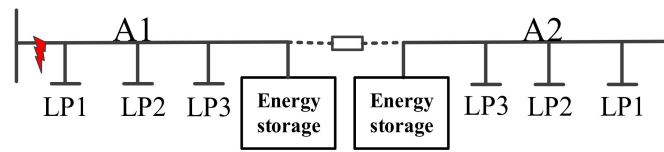


Figure 5. The fault diagram of the feeders group.

The upgrading of distribution networks slows down effectively, because GDSRs in the feeders group reduces the peak of the load curve and improves the line safety load rate. Therefore, the income from the delay of distribution networks upgrading is determined by the peak load reduction and the increase of the safety load rate after GDSRs are allocated. The specific calculation method is shown as follows.

In this paper, let ε be the annual growth rate of the load, where $\eta_{p.max}$ and $\eta_{n.max}$ are the safety load rate of the line before and after the GDSRs are allocated, respectively. $P_{p.max}$ and $P_{n.max}$ are the peak of the load curve before and after the GDSRs are allocated, respectively. T_p and T_n are the years from now to the grid upgrade before and after the GDSRs are allocated, respectively. The equation can be shown in (6).

$$\begin{aligned} P_{n.max}(1 + \varepsilon)^{T_n} &= \eta_{n.max}P_T \\ P_{p.max}(1 + \varepsilon)^{T_p} &= \eta_{p.max}P_T \end{aligned} \tag{6}$$

In the formula, P_T represents the rated transmission power of the distribution networks.

According to the Formula (6), the equation for the years of deferring grid upgrade T_{del} can be shown in (7).

$$T_{del} = [\lg(\frac{\eta_{n.max}}{\eta_{p.max}}) - \lg(\frac{P_{n.max}}{P_{p.max}})] \frac{1}{\lg(1 + \varepsilon)} \tag{7}$$

Here is the specific calculation of $\eta_{n.max}$ in Formula (7). After transforming the energy storage equivalent to a negative load, set a 50% load factor as the starting point and increase the line load rate gradually. Then, check whether the line meets the constraint of the power flow and the voltage when accepting all of the transferred load from the opposite line. When the load rate grows to the point which is no longer satisfied by the constraint, the critical load rate is $\eta_{n.max}$.

Therefore, through the coordinated dispatching and sharing GDSRs in the feeders group, the profits of delaying the grid upgrade can be shown in (8).

$$B_{del} = I_{dis} [1 - (\frac{1 + i_r}{1 + d_r})^{\frac{1}{\lg(1 + \varepsilon)} [\lg(\frac{\eta_{n.max}}{\eta_{p.max}}) - \lg(\frac{P_{n.max}}{P_{p.max}})]}] \tag{8}$$

In the formula, I_{dis} represents the investment of the grid upgrade. i_r is the inflation rate. d_r is the discount rate.

3.1.2. The Profits of Reliability Improvement

Under the fault state of distribution networks, energy storage can supply power for the load inside the planned island when the faulty element is located within the planned island. Therefore, it can improve the reliability. This part of the profit is the income from the reduced amount of compensation paid by the DisCo due to the users' power outage. This paper selects the failure consequence analysis method to calculate the profits. The formula is shown in (9).

$$\begin{aligned} B_{rel} &= \sum_{t=1}^{t_{total}} [(\sum_{j=1}^{N_{fault}} E_j) (\frac{1+i_r}{1+d_r})^t] \\ E_j &= \min(\sum_{i=1}^{N_{fault.load}} P_i r_j \omega_{j,r} S_{res}) \frac{\lambda_j}{\lambda_j + \mu_j} R_{rea} \end{aligned} \tag{9}$$

In the formula, N_{fault} represents the number of elements inside the planned island. E_j represents the reduced expectation of power loss due to the energy storage supply power for the load inside the planned island when the j -th element is in fault mode. $N_{fault.load}$ represents the number of loads inside the planned island. P_i represents the power required to secure the user's power supply. r_j represents the average duration of the j -th element failure. $\omega_{j,i}$ represents that the energy storage in the island can supply power for the k -th users when the j -th component fails. When the supply path exists, $\omega_{j,i}$ is 1 or 0. S_{res} indicates the expected surplus power in the energy storage when the grid is in fault mode. λ_j, μ_j represent the failure rate and repair rate of the j -th element, respectively. R_{rea} represents the evaluation rate of the users' lack of electricity.

3.2. Restrictions

(1) The constraint of the system active power balance

$$P_{BES,t} + P_{tran,t} + \sum_{i \in N_{DG}} p_{DG_i,t} = \sum_{i \in N} p_{load_i,t} + p_{loss,t} \quad (10)$$

In the formula, $p_{BES,t}$ represents the output of energy storage at time t . $p_{DG_i,t}$, $p_{tran,t}$, and $p_{load_i,t}$ represent the output of PV, the electricity bought from the transmission grid, and the load power of load point i at time t , respectively. $p_{loss,t}$ represents the network loss of distribution networks. N represents the total number of load nodes in distribution networks. N_{DG} represents the number of nodes of the users allocating PV.

(2) The constraint of voltage

$$U_{\min} \leq U_i \leq U_{\max} \quad (11)$$

In the formula, U_i represents the voltage of node i . U_{\min} and U_{\max} represent the lower and higher limit of the voltage, respectively.

(3) The constraint of input power

$$0 \leq P_{tran,t} \leq P_{tran,max} \quad (12)$$

In the formula, $p_{tran,max}$ represents the upper limit of the power transferred from the transmission networks to the distribution networks.

(4) The bound of upper and lower price

$$C_{\min} < C(k) < C_{\max} \quad (13)$$

In the formula, C_{\min} and C_{\max} represent the upper and lower limits of the electricity price determined by the relevant departments, respectively.

(5) The bound of upper and lower price mean

$$C_{mean,min} < \frac{1}{48} \sum_{k=1}^{48} C(k) < C_{mean,max} \quad (14)$$

In the formula, $C_{mean,min}$ and $C_{mean,max}$ represent the upper and lower limits of the electricity price mean, respectively, to ensure the volatility of the price optimization results. In this paper, the upper and lower limits are 0.9 RMB/kW·h and 1.1 RMB/kW·h, respectively.

4. The Solution of Planning Model Based on Operation Simulation

This paper solved the planning model through the tabu search-particle swarm algorithm (TS-PSO) [22] and typical daily operation scheduling simulation. The TS-PSO algorithm introduced the thought of "taboo" and "amnesty" into the search update of the particle swarm algorithm, and solved the problem of a weak local search ability and premature convergence in the PSO algorithm.

This algorithm not only speeds up the convergence rate, but also improves the convergence accuracy. The concrete flow of the model is shown in Figure 6.

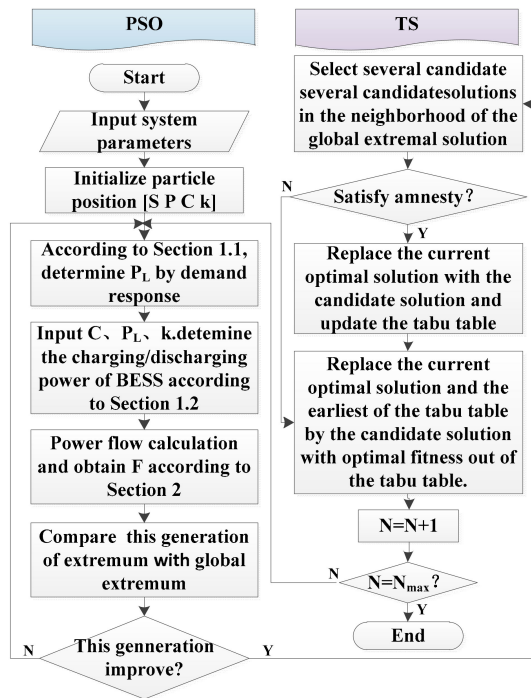


Figure 6. The specific process of solving the model.

5. Results

This paper takes the ‘hand in hand’ feeders group composed of two identical improved IEEE-33 bus test systems as an example to analyse the model. In the test system, node 10, 20, 24, and 28 are selected as large commercial users to configure USRT and PV, and node 18 is set as the position of energy storage configuration. One of the feeders is shown in Figure 7. The impedance of each distribution line in the IEEE-33 bus system used in the case study is shown in Appendix B, Table A2.

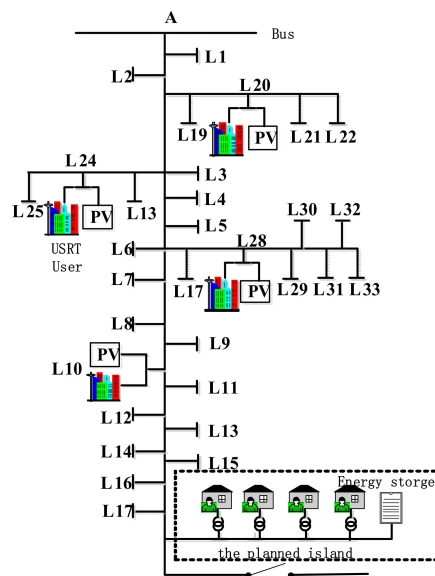


Figure 7. Modified IEEE-33 nodes distribution system.

5.1. Initial Parameter

This paper takes the annual load growth rate as 1.2%. The baseline load curve after calculation is shown in Figure 8. The electricity price of the power buying from transmission networks is set as a single price. The demand-side electricity price from 7:00 to 22:00 is variable to be optimized, whilst the price at the other time is 0.7 RMB/kWh. Inflation is set as 1.6%. The discount rate is set as 10%. The evaluation rate of the users' lack of electricity is 1355 RMB/kWh. The air condition parameters of the commercial users are set according to Reference [23]. The users' demand for temperature is set as 27–22 °C. The parameters of energy storage are set according to Reference [9]. The reliability data of the components in the example are set according to Reference [24].

This paper divides one year into six equal periods, and selects the temperature in a typical day from each period as the research scene. The temperature in a typical day is shown in Figure 9.

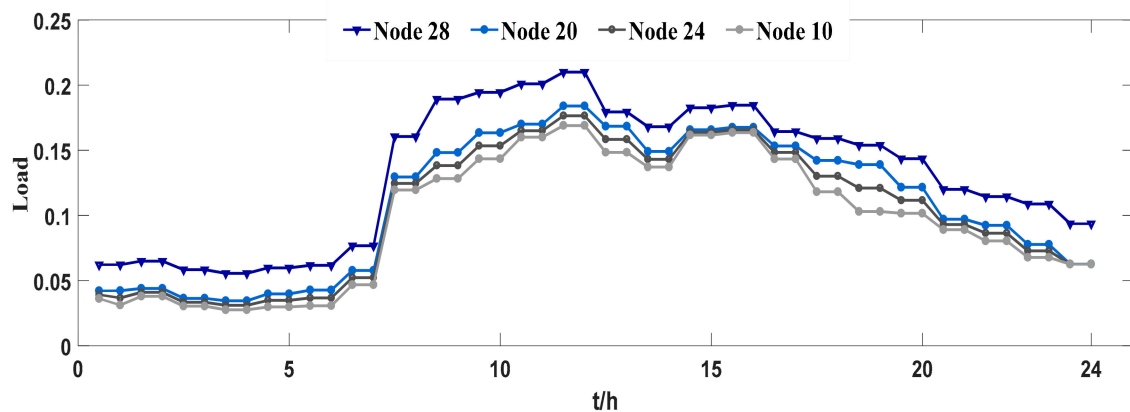


Figure 8. Load of the user baseline.

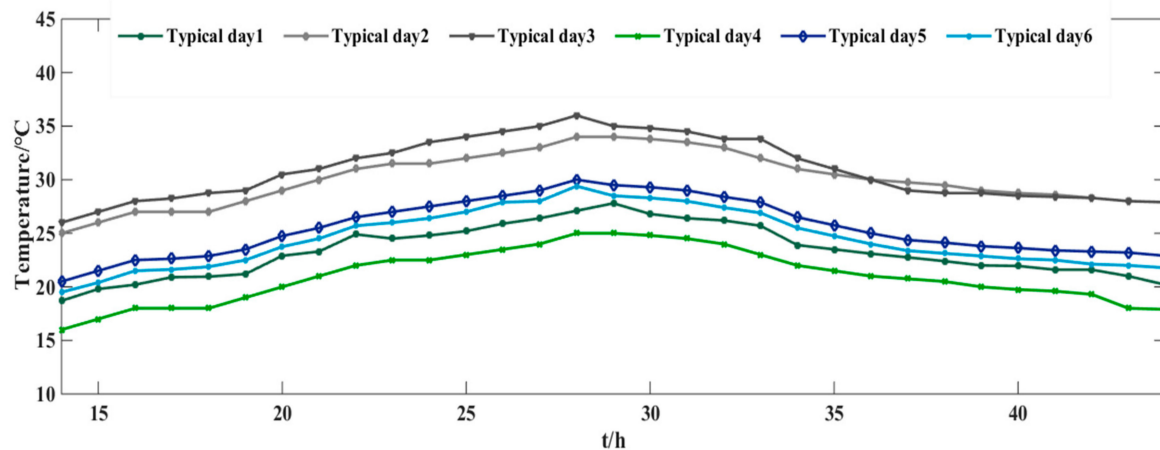


Figure 9. Temperature of the typical days.

The parameter of the algorithm is set as follows. The number of iteration times is 1000. The number of population sizes is 50. The particle dimension is 37. The weight coefficient of the particle tracking its historical optimal value is 2. The weight coefficient of the particle tracking group optimal value is 2. The constraint factor is 0.729.

According to the data above, the convergent results after optimization are as follow: $k_{c,max} = 0$, $k_{c,min} = 0$, $k_{l,max} = 0.6826$, $k_{l,min} = 0.4243$, $SOC_{min} = 0.24$, $S_{es} = 7021$ kWh, $P_{es} = 559.077$ kW. The optimization results of the demand-side electricity price are shown in Figure 10.

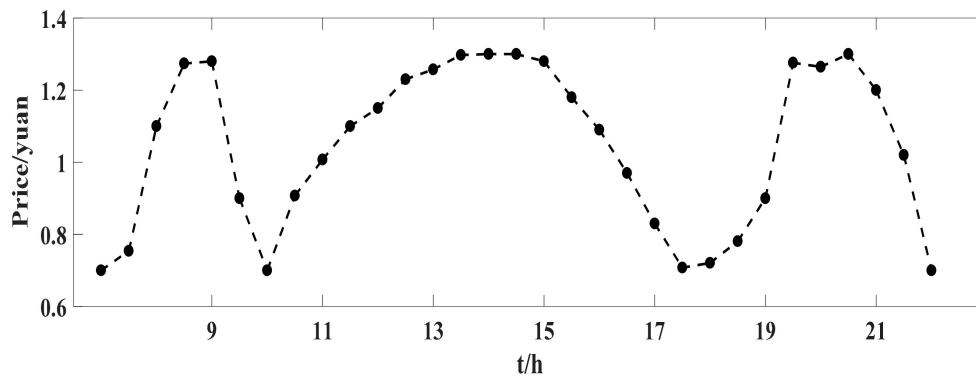


Figure 10. The optimization results of the demand-side electricity price.

5.2. The Impact of the Demand Side Response to Users

(1) Impact on users' comfort

When the USRT responds to the demand-side electricity price, the users' indoor temperature are shown in Figure 11.

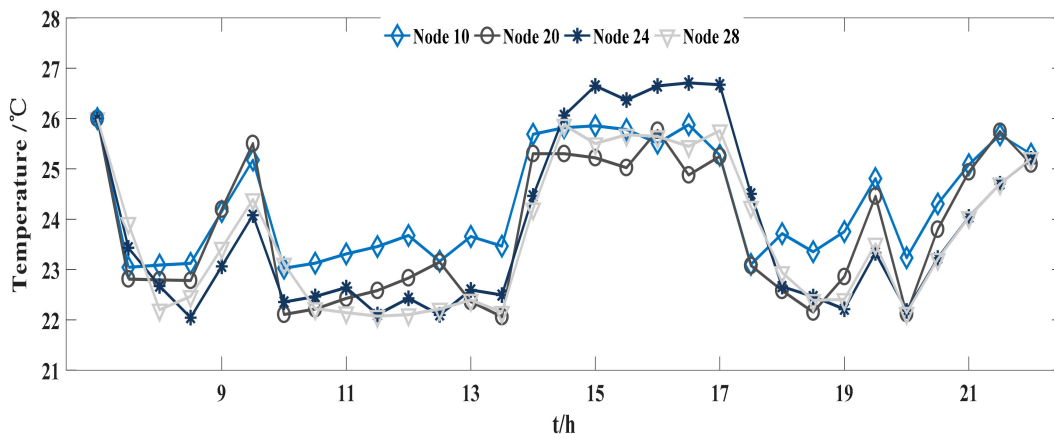


Figure 11. The temperature response results of USRT.

From the Figure 11, the response results of USRT meet the users' temperature requirements. The impact of the outdoor temperature and the electricity price result in the temperature curve of different users showing similar trends.

(2) Impact on the economic efficiency of users

In order to analyze the economic efficiency of users' participation in response, we compared the annual electricity costs of the air condition (Unit: 10 thousand) between the control method proposed in this paper (Method 1) and the start and stop control method (Method 2) of the air condition under the same price. In Method 2, the state of the air condition is determined by whether the temperature is beyond the users' satisfied temperature range. The specific results are shown in Figure 12.

From Figure 12, the cost of the users' air condition under Method 1 is low, so the users' economic efficiency improves. Among these users, the reduction rates of the users' electricity cost of Node 10, 20, 24, and 28 are 9.4%, 9.2%, 9.1%, and 10.4%, respectively. The reduction rate of the users' electricity cost of Node 28 is the highest, which also has the maximum rated power of the air condition. It shows that the reduction rate of the users' electricity costs and the rated power of the users' air condition are positively correlated.

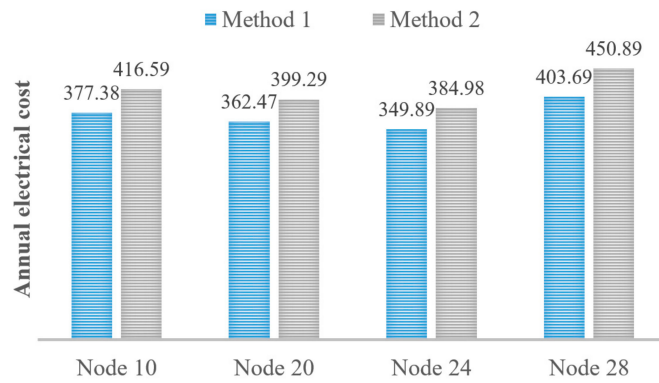


Figure 12. The comparison of user electricity costs.

5.3. The Impact of Demand Side Resource Configuration on Energy Storage Configuration

On the basis of keeping other parameters constant, gradually change the proportion of important users who participate in the response. The optimization results of the energy storage operation and configuration are shown in Figure 13.

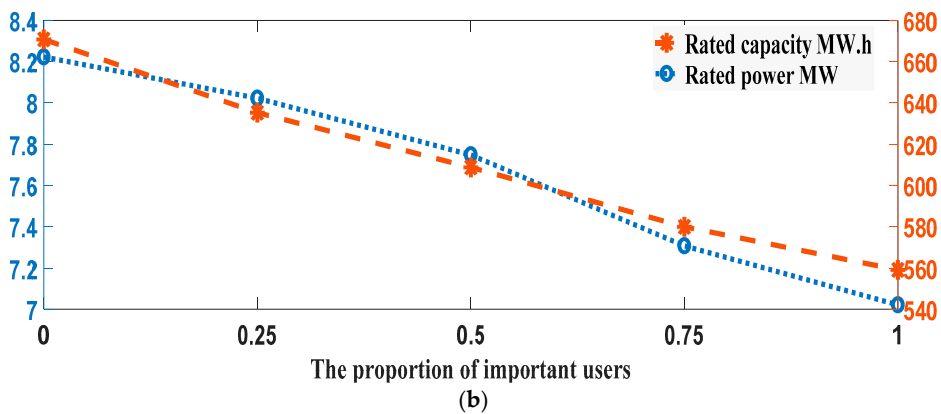
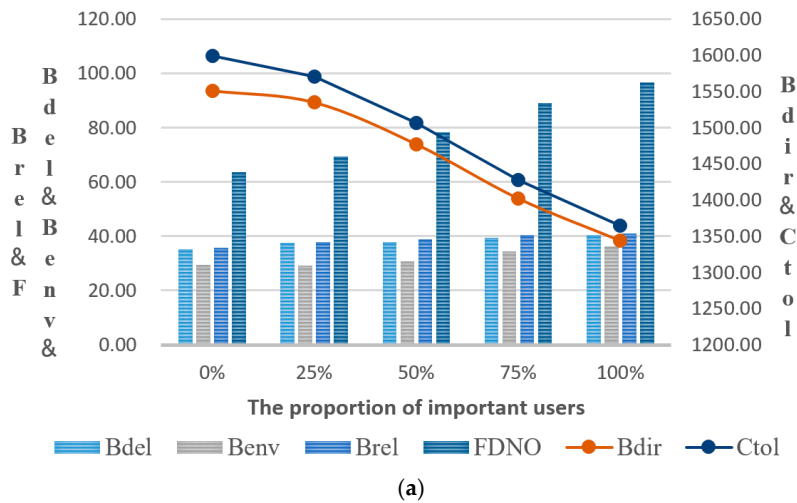


Figure 13. Energy storage configuration results under different user load demand response participation rates. (a) Indicated the results of the incomes and the cost; (b) indicated the results of the rated capacity and power.

From Figure 13, as the proportion of users participating in the demand side increases, the energy storage rated capacity and rated power decrease. At the same time, the configuration cost and the

direct benefit of the DisCo reduce. This is because the direct benefits are proportional to the energy storage rated capacity. When the users participate in the response, the peak and valley characteristics of the load curve has been adjusted. So, the cost of energy storage configuration and the direct benefits are reduced. However, because the profits from delaying the upgrade of distribution networks, the environmental benefits, and the profits of reliability improvement increase with the increase of the proportion of users who participate in the response, the DisCo net income increases.

5.4. The Effect of PV Permeability on Energy Storage Allocation

This section takes into account the restrictions on the PV capacity configured in the commercial users, and analyzes the influence of the parameter changes on the energy storage configuration. The results of energy storage allocation is shown in Table 1.

Table 1. The results of BESS configuration.

PV Permeability	$S_{es}/(\text{MW}\cdot\text{h})$	P_{es}/kW	F
0.1	7.021	559.077	96.668
0.15	6.473	528.247	100.422
0.2	5.978	493.978	104.023
0.25	5.525	464.505	107.055
0.3	5.113	428.177	110.450

Within the scope of analysis, S_{es} and P_{es} reduce, and F increases with the increase of PV permeability. Because the curve of the PV output and user load have a similar time characteristic, PV configuration can optimize the load characteristics and reduce the requirements of energy storage configuration, which reduces the configuration costs and increases the net income of the DisCo.

5.5. The Influence of GDSRs on the Safety Load Rate under Shared Mechanism

In order to analyze the effect of the GDSRs operation strategy on the safety load rate of the line, the safety load rate of the line is calculated as shown in Table 2 under different configurations of GDSRs.

Table 2. The Influence of GDSRs on the Safety Load Rate.

Energy Storage Configuration		✓	✓	✓	✓	✓
The proportion of important users	0%	0%	25%	50%	75%	100%
The safety load rate of the line	50%	54.66%	55.51%	56.25%	56.93%	57.7%

As can be seen from Table 2, with the increase of the energy storage configuration and the proportion of users participating in the response, the safety load rate of the line gradually increases. Because the transfer load that the energy storage can undertake is higher, the improvement of it is more significant to the safety load rate of the line. It shows that the improvement of the line safety load rate has a positive correlation with the scale of the GDSRs configuration.

6. Conclusions

In this paper, the optimal configuration of the energy storage capacity under the resource sharing mechanism of a generalized demand side is studied, with the aim of maximizing the economic benefits obtained by the DisCo. The optimization process in this paper takes into account the configuration and operating parameter. This paper also considers the different operational strategies of GDSRs under the normal state and the fault state, and achieves the unity of the application scene, the main investment, construction goals, and operational strategy. The following can be shown by the case study. (1) The model built in this paper satisfies the demands of the users' comfort and economic efficiency; (2) Requirements of energy storage configuration decreases as the proportion of users participating in the demand side increases; (3) The increase of PV permeability within the scope can

decrease the requirements of energy storage configuration and increase the net income of the DisCo; (4) The configuration and sharing of the general demand side resource in the feeders group improves the safety load rate of the line, and its promotion effect is positively correlated with the configuration scale. It is worth noting that although the optimization is carried out on the improved IEEE-33 bus test system, the optimization has no limit on the number of system nodes.

The research content of this paper can provide a reference for the planning and utilization of GDSRs, the optimization of the operation strategy of energy storage, and the formulation of the real-time electricity price.

Acknowledgments: This work is supported by National key research and development program of China (2017YFB0903103).

Author Contributions: Wenxia Liu designed, directed, and made suggestions for this research. Shu Wang was responsible for the experiments, analyzed the data, and wrote this paper. Lingfei Wang, Xingliang Chen, and Shuya Niu took part in the revision work. All authors have read and approved the final manuscript.

Conflicts of Interest: The authors declare no conflict of interest.

Nomenclature

Indices:

t	Index for planning time stage
k	Index for response period
Δk	Index for time interval in the response
i	Index of users load nodes
j	Index of elements in distribution network

Sets:

Q_k	Set of candidate choices of air condition stalls in the k -th period
-------	--

Parameters:

T_{in}	Indoor temperature
T_{out}	Outdoor temperature
R	Thermal resistance parameter
C	Equivalent heat capacity parameters
P	Rated cooling/heating power of air condition
η	Performance parameters of air condition
q	Five power stalls of the air condition
P_v	Users' PV output
$N_{transfer}$	The amount of elements in distribution network
r	The average duration of element failure
R_a	Lack of power supply evaluation rate
λ	The failure rate of the element
μ	The repair rate of the element
I_{dis}	The investment required for the grid upgrade
U_{max}	The higher voltage limit
U_{min}	The lower voltage limit
$p_{tran,max}$	The upper limit of power transferred from the transmission grid to the distribution grid

Variables:

$k_{c,max}$	The transmission grid price upper limit parameter
$k_{c,min}$	The transmission grid price lower limit parameter
$k_{l,max}$	The user load upper limit parameter
$k_{l,min}$	The user load lower limit parameter
C	Distribution network electricity price
η	The safety load rate of the line
P_{max}	The peak of the load curve
SOC_{min}	The lower limit of SOC
S_{es}	The rated capacity of energy storage
P_{es}	The power of energy storage

i_r	The inflation rate
d_r	The discount rate
B_{dir}	The direct return of the DisCo
B_{del}	The profit of delaying the upgrading of distribution networks
B_{env}	The environmental benefits
B_{rel}	The profit of reliability improvement
C_{tol}	The energy storage life cycle cost
C_{dsm}	The economic compensation for the users

Appendix A

The list of abbreviations used in this manuscript is shown in Table A1.

Table A1. List of abbreviations.

Abbreviations	Full Name
RERs	renewable energy resources
DisCo	distribution company
GDSRs	generalized demand side resources
DWG	distributed wind generation
PV	solar photovoltaic
DG	distributed generation
SOC	state of charge

Appendix B

The impedance of each distribution line in the IEEE-33 bus system used in the case study is shown in Table A2.

Table A2. IEEE-33 bus system data.

Sending Node	Receiving Node	Resistance (Ohm)	Reactance (Ohm)
1	2	0.0575	0.0293
2	3	0.3076	0.1567
3	4	0.2284	0.1163
4	5	0.2378	0.1211
5	6	0.5109	0.4411
6	7	0.1168	0.3861
7	8	0.4439	0.1467
8	9	0.6426	0.4617
9	10	0.6514	0.4617
10	11	0.1227	0.0406
11	12	0.2336	0.0772
12	13	0.9159	0.7206
13	14	0.3379	0.4448
14	15	0.3687	0.3282
15	16	0.4656	0.34
16	17	0.8042	1.0738
17	18	0.4567	0.3581
2	19	0.1023	0.0976
19	20	0.9385	0.8457
20	21	0.2555	0.2985
21	22	0.4423	0.5848
3	23	0.2815	0.1924
23	24	0.5603	0.4424
24	25	0.5591	0.4374
8	26	0.1267	0.0645
26	27	0.1773	0.0903
27	28	0.6607	0.5826
28	29	0.5018	0.4371
29	30	0.3166	0.1613
30	31	0.6079	0.6008
31	32	0.1937	0.2258
32	33	0.2128	0.3308
8	21	1.25	1.25
9	15	1.25	1.25
12	22	1.25	1.25
18	33	0.3125	0.3125
24	29	0.3125	0.3125

References

1. Senjyu, T.; Miyazato, Y.; Yona, A.; Urasaki, N.; Funabashi, T. Optimal distribution voltage control and coordination with distributed generation. *IEEE Trans. Power Deliv.* **2008**, *23*, 1236–1242. [[CrossRef](#)]
2. Han, X.; Liao, S.; Ai, X.; Yao, W.; Wen, J. Determining the Minimal Power Capacity of Energy Storage to Accommodate Renewable Generation. *Energies* **2017**, *10*, 468. [[CrossRef](#)]
3. Xu, X.; Huang, Y.; Liu, C.; Wang, W. Influence of Distributed Photovoltaic Generation on Voltage in Distribution Network and Solution of Voltage beyond Limits. *Power Syst. Technol.* **2010**, *10*, 140–146.
4. Hadjsaid, N.; Canard, J.F.; Dumas, F. Dispersed generation impact on distribution networks. *IEEE Comput. Appl. Power* **2002**, *12*, 22–28. [[CrossRef](#)]
5. Zhou, Y.; Mancarella, P.; Mutale, J. Framework for capacity credit assessment of electrical energy storage and demand response. *IET Gener. Transm. Distrib.* **2016**, *10*, 2267–2276. [[CrossRef](#)]
6. Telaretti, E.; Graditi, G.; Ippolito, M.G.; Zizzo, G. Economic feasibility of stationary electrochemical storages for electric bill management applications: The Italian scenario. *Energy Policy* **2016**, *94*, 126–137. [[CrossRef](#)]
7. Sanseverino, E.R.; Silvestre, M.L.D.; Zizzo, G.; Gallea, R.; Quang, N.N. A Self-Adapting Approach for Forecast-Less Scheduling of Electrical Energy Storage Systems in a Liberalized Energy Market. *Energies* **2013**, *6*, 5738–5759. [[CrossRef](#)]
8. Zhong, Q.; Yu, N.; Zhang, X.; Yi, Y.; Dong, L. Optimal Siting & Sizing of Battery Energy Storage System in Active Distribution Network. In Proceedings of the IEEE Innovative Smart Grid Technologies Europe, Copenhagen, Denmark, 6–9 October 2013; pp. 1–5.
9. Chakraborty, S.; Senjyu, T.; Toyama, H.; Saber, A.Y.; Funabashi, T. Determination methodology for optimising the energy storage size for power system. *IET Gener. Transm. Distrib.* **2009**, *3*, 987–999. [[CrossRef](#)]
10. Liu, W.; Niu, S.; Xu, H. Optimal planning of battery energy storage considering reliability benefit and operation strategy in active distribution system. *J. Mod. Power Syst. Clean Energy* **2017**, *5*, 177–186. [[CrossRef](#)]
11. Palensky, P.; Dietrich, D. Demand Side Management: Demand Response, Intelligent Energy Systems, and Smart Loads. *IEEE Trans. Ind. Inf.* **2011**, *7*, 381–388. [[CrossRef](#)]
12. Asensio, M.; Quevedo, P.M.D.; Munoz-Delgado, G.; Contreras, J. Joint Distribution Network and Renewable Energy Expansion Planning considering Demand Response and Energy Storage Part I: Stochastic Programming Model. *IEEE Trans. Smart Grid* **2016**. [[CrossRef](#)]
13. Marwan, M.; Ledwich, G.; Ghosh, A. Smart Grid-Demand Side Response Model for Optimization Air Conditioning. In Proceedings of the IEEE Universities Power Engineering Conference, Bali, Indonesia, 26–29 September 2012; pp. 1–6.
14. Zhu, L.; Yan, Z.; Yang, X. Integrated Resources Planning in Microgrid Based on Modeling Demand Response. *Proc. CSEE* **2014**, *16*, 2621–2628.
15. Zhou, Y. Generalized demand side resources for microgrid energy management. In Proceedings of the 2014 IEEE PES Asia-Pacific Power and Energy Engineering Conference (APPEEC), Hong Kong, China, 7–10 December 2014; pp. 1–6.
16. Tang, Q.; Liu, N.; Zhang, J. Theory and key problems for automated demand response of user side considering generalized demand side resources. *Power Syst. Prot. Control* **2014**, *24*, 138–147.
17. Liu, Y.; Yang, Z.; Xiu, J.; Liu, C. Research on an anti-crawling mechanism and key algorithm based on sliding time window. In Proceedings of the 2016 4th International Conference on Cloud Computing and Intelligence Systems (CCIS), Beijing, China, 17–19 August 2016; pp. 220–223.
18. Lu, N. An evaluation of the HVAC load potential for providing load balancing service. *IEEE Trans. Smart Grid* **2012**, *3*, 1263–1270. [[CrossRef](#)]
19. Asadinejad, A.; Tomsovic, K. Impact of Incentive Based Demand Response on large scale renewable integration. In Proceedings of the 2016 IEEE Power & Energy Society Innovative Smart Grid Technologies Conference (ISGT), Minneapolis, MN, USA, 6–9 September 2016; pp. 1–5.
20. Shen, X.; Shahidehpour, M.; Han, Y.; Zhu, S.; Zheng, J. Expansion Planning of Active Distribution Networks with Centralized and Distributed Energy Storage Systems. *IEEE Trans. Sustain. Energy* **2017**, *8*, 126–134. [[CrossRef](#)]
21. Yuan, Y.; Li, Q.; Wang, W. Optimal operation strategy of energy storage unit in wind power integration based on stochastic programming. *IET Renew. Power Gener.* **2011**, *5*, 194–201. [[CrossRef](#)]

22. Guo, H.; Lan, R.; Chen, X.; Wang, Y.X. Tabu search-particle swarm algorithm for protein folding prediction. *Comput. Eng. Appl.* **2011**, *47*, 46–50.
23. Gao, C.; Li, Q.; Li, Y. Bi-level optimal dispatch and control strategy for air-conditioning load based on direct load control. *Proc. CSEE* **2014**, *34*, 1546–1555.
24. Wan, G.C.; Ren, Z.; Tian, X. Study on model of reliability-network-equivalent of distribution system reliability evaluation. *Proc. CSEE* **2003**, *5*, 011.



© 2017 by the authors. Licensee MDPI, Basel, Switzerland. This article is an open access article distributed under the terms and conditions of the Creative Commons Attribution (CC BY) license (<http://creativecommons.org/licenses/by/4.0/>).